TABLE 2. Correlation Between Visual Function and Parallelism of Retinal Layers in Optical Coherence Tomographic Images in Patients With Epiretinal Membrane

	Horizontal Scan			Vertical Scan		
	M-CHARTS Horizontal Metamorphopsia Score	M-CHARTS Vertical Metamorphopsia Score	Visual Acuity (LogMAR)	M-CHARTS Horizontal Metamorphopsia Score	M-CHARTS Vertical Metamorphopsia Score	Visual Acuity (LogMAR)
Parallelism full thickness						
6 mm	$P < .0001$; $R = -0.543$	$P = .0003$; $R = -0.482$	$P = .0016$; $R = -0.434$	$P = .0012$; $R = -0.453$	$P < .0001$; $R = -0.533$	$P = .0024$; $R = -0.428$
T or I, 1.5-3.0 mm	$P = .0063$; $R = -0.383$	$P = .0052$; $R = -0.391$	$P = .0257$; $R = -0.318$	$P = .1487$; $R = -0.214$	$P = .0012$; $R = -0.453$	$P = .4462$; $R = -0.114$
T or I, 0.5-1.5 mm	$P = .0002$; $R = -0.499$	$P = .0023$; $R = -0.421$	$P = .0050$; $R = -0.392$	$P = .0008$; $R = -0.465$	$P = .0001$; $R = -0.524$	$P = .0064$; $R = -0.389$
Center, 1.0 mm	$P < .0001$; $R = -0.632$	$P = .0003$; $R = -0.487$	$P < .0001$; $R = -0.522$	$P = .0035$; $R = -0.414$	$P = .0009$; $R = -0.462$	$P = .0018$; $R = -0.439$
N or S, 0.5-1.5 mm	$P = .0036$; $R = -0.404$	$P = .0220$; $R = -0.325$	$P = .0206$; $R = -0.329$	$P = .0074$; $R = -0.383$	$P = .0024$; $R = -0.428$	$P = .0292$; $R = -0.317$
N or S, 1.5-3.0 mm	$P = .1106$; $R = -0.231$	$P = .0148$; $R = -0.345$	$P = .0738$; $R = -0.258$	$P = .0184$; $R = -0.341$	$P = .0250$; $R = -0.326$	$P = .0061$; $R = -0.392$
Parallelism inner layer						
T or I, 1.5-3.0 mm	$P = .0052$; $R = -0.391$	$P = .0022$; $R = -0.422$	$P = .0445$; $R = -0.288$	$P = .0764$; $R = -0.261$	$P = .0026$; $R = -0.425$	$P = .4522$; $R = -0.113$
T or I, 0.5-1.5 mm	$P = .0004$; $R = -0.483$	$P = .0070$; $R = -0.378$	$P = .0139$; $R = -0.348$	$P = .0017$; $R = -0.440$	$P = .0007$; $R = -0.469$	$P = .0132$; $R = -0.357$
Center, 1.0 mm	$P < .0001$; $R = -0.621$	$P = .0034$; $R = -0.407$	$P = .0006$; $R = -0.466$	$P = .0040$; $R = -0.409$	$P = .0038$; $R = -0.410$	$P = .0077$; $R = -0.381$
N or S, 0.5-1.5 mm	$P = .0016$; $R = -0.435$	$P = .0255$; $R = -0.318$	$P = .0233$; $R = -0.322$	$P = .0163$; $R = -0.347$	$P = .0103$; $R = -0.369$	$P = .0581$; $R = -0.278$
N or S, 1.5-3.0 mm	$P = .0370$; $R = -0.298$	$P = .0570$; $R = -0.273$	$P = .0348$; $R = -0.302$	$P = .0131$; $R = -0.357$	$P = .0434$; $R = -0.295$	$P = .0071$; $R = -0.385$
Parallelism outer layer						
T or I, 1.5-3.0 mm	$P = .2754$; $R = -0.159$	$P = .0098$; $R = -0.363$	$P = .0388$; $R = -0.296$	$P = .4314$; $R = -0.118$	$P = .0421$; $R = -0.297$	$P = .9934$; $R = 0.001$
T or I, 0.5-1.5 mm	$P = .0568$; $R = -0.274$	$P = .0161$; $R = -0.341$	$P = .0198$; $R = -0.331$	$P = .0386$; $R = -0.302$	$P = .0010$; $R = -0.460$	$P = .0313$; $R = -0.314$
Center, 1.0 mm	$P = .0232$; $R = -0.323$	$P = .0160$; $R = -0.341$	$P = .0345$; $R = -0.302$	$P = .4311$; $R = -0.118$	$P = .5334$; $R = -0.094$	$P = .0700$; $R = -0.267$
N or S, 0.5-1.5 mm	$P = .3061$; $R = -0.150$	$P = .4339$; $R = -0.115$	$P = .3828$; $R = -0.128$	$P = .0470$; $R = -0.291$	$P = .0097$; $R = -0.371$	$P = .3365$; $R = -0.144$
N or S, 1.5-3.0 mm	$P = .7090$; $R = -0.055$	$P = .8746$; $R = 0.023$	$P = .6622$; $R = -0.064$	$P = .4689$; $R = 0.109$	$P = .8523$; $R = 0.028$	$P = .4219$; $R = 0.120$
Retinal thickness						
T or I, 1.5-3.0 mm	$P = .1261$; $R = 0.222$	$P = .2462$; $R = 0.169$	$P = .1106$; $R = 0.231$	$P = .3699$; $R = 0.134$	$P = .2903$; $R = 0.158$	$P = .0581$; $R = 0.278$
T or I, 0.5-1.5 mm	$P = .0009$; $R = 0.454$	$P = .0027$; $R = 0.416$	$P = .0059$; $R = 0.385$	$P = .0201$; $R = 0.337$	$P = .0076$; $R = 0.382$	$P = .0007$; $R = 0.472$
Center, 1.0 mm	$P = .0031$; $R = 0.410$	$P = .0078$; $R = 0.373$	$P = .0011$; $R = 0.447$	$P = .0018$; $R = 0.438$	$P = .0218$; $R = 0.333$	$P = .0004$; $R = 0.486$
N or S, 0.5-1.5 mm	$P = .1626$; $R = 0.203$	$P = .1231$; $R = 0.223$	$P = .0137$; $R = 0.348$	$P = .2168$; $R = 0.184$	$P = .2289$; $R = 0.179$	$P = .0026$; $R = 0.426$
N or S, 1.5-3.0 mm	$P = .2910$; $R = 0.154$	$P = .5059$; $R = 0.098$	$P = .1166$; $R = 0.227$	$P = .2663$; $R = 0.166$	$P = .2208$; $R = 0.183$	$P = .0034$; $R = 0.415$

ERM = epiretinal membrane; I = inferior; LogMAR = logarithm of minimal angle of resolution; N = nasal; S = superior; T = temporal.

TABLE 3. Correlation Between Parallelism of Retinal Layers and Retinal Thickness in Optical Coherence Tomographic Images of Patients With Epiretinal Membrane

	Parallelism		
	Full Thickness	Inner Layers	Outer Layers
Retinal thickness, horizontal scan			
Temporal, 1.5-3.0 mm	$P < .0001$; $R = -0.608$	$P < .0001$; $R = -0.614$	$P = .0138$; $R = -0.348$
Temporal, 0.5-1.5 mm	$P < .0001$; $R = -0.720$	$P < .0001$; $R = -0.720$	$P = .0008$; $R = -0.456$
Center, 1 mm	$P < .0001$; $R = -0.701$	$P < .0001$; $R = -0.690$	$P = .0447$; $R = -0.288$
Nasal, 0.5-1.5 mm	$P < .0001$; $R = -0.673$	$P < .0001$; $R = -0.662$	$P = .0185$; $R = -0.334$
Nasal, 1.5-3.0 mm	$P < .0001$; $R = -0.541$	$P = .0002$; $R = -0.505$	$P = .5717$; $R = -0.083$
Retinal thickness, vertical scan			
Inferior, 1.5-3.0 mm	$P < .0001$; $R = -0.551$	$P = .0002$; $R = -0.516$	$P = .0008$; $R = -0.467$
Inferior, 0.5-1.5 mm	$P < .0001$; $R = -0.617$	$P < .0001$; $R = -0.528$	$P = .0030$; $R = -0.419$
Center, 1 mm	$P < .0001$; $R = -0.601$	$P < .0001$; $R = -0.609$	$P = .1477$; $R = -0.215$
Superior, 0.5-1.5 mm	$P < .0001$; $R = -0.633$	$P < .0001$; $R = -0.606$	$P = .0655$; $R = -0.271$
Superior, 1.5-3.0 mm	$P < .0001$; $R = -0.608$	$P < .0001$; $R = -0.640$	$P = .8814$; $R = 0.022$

of structural changes in OCT images of ERM. Results from multiple linear regression analysis showed that parallelism in both the horizontal and vertical scans contributed most to the horizontal and vertical metamorphopsia scores, implying that parallelism correlated with metamorphopsia score better than did retinal thickness.

Parallelism represents the positional relationship among line segments rather than retinal thickness. Although our selection of the parameter parallelism was first based on its potential to evaluate retinal layer integrity using the full thickness of the retina instead of local layer thickness, we challenged our results by also evaluating its usefulness in the inner and outer layers in the current study. As a result, inner-layer parallelism correlated strongly with metamorphopsia score and visual acuity, while outer-layer parallelism had a modest relationship with these visual functions, suggesting that the contribution made by the parallelism of the inner layer to visual function was greater than that made by the outer layer in this study.

A number of studies have reported relationships between retinal morphologic features and metamorphopsia in ERM. Watanabe and associates,[34] Kim and associates,[14] and Okamoto and associates[13] used SDOCT and reported a significant relationship between inner nuclear layer thickness and metamorphopsia. Arimura and associates investigated the relationship between the degree of retinal contraction and the degree of metamorphopsia, and found that there were significant positive correlations between horizontal contraction of the retina and vertical metamorphopsia score and between vertical contraction of the retina and horizontal metamorphopsia score.[35] Collectively, these studies suggest that metamorphopsia in patients with ERM associates with pathologic changes in the inner layer of the retina but not with photoreceptor status. Our results also showed that parallelism of the inner layer correlated strongly with metamorphopsia score. However, Ooto and associates described that eyes with ERM showed abnormal photoreceptor cone mosaic patterns and found that the presence of "microfolds" (a characteristic finding that might correspond to contraction in the photoreceptor layer caused by shrinkage of the ERM) was associated with metamorphopsia by using adaptive-optics scanning laser ophthalmoscopy images, which suggested involvement of the photoreceptor layer in metamorphopsia.[24] In our study, parallelism in the outer layer in both horizontal and vertical scans showed modest correlations with horizontal or vertical metamorphopsia score. Thus, parallelism in the outer layer may have the potential of reflecting the photoreceptor integrity.

A classical digital filtering process was used to generate skeletonized images for calculation of parallelism in this study.[28–30] The benefits of image analysis based on a simple filtering process are its low computational complexity and faithfulness to the original images without segmentation failure. However, as stated before, extraction of structures other than the boundaries of retinal layers, such as vessels and vessel shadows in the vertical scan, might be considered flaws. On the other hand, considering that parallelism can represent changes in the layered structure, parallelism may have the potential to automatically detect abnormal findings in OCT images even in cases with normal retinal thickness. Moreover, parallelism can be used as a parameter of complexity of images, thereby enabling quantification of complicated findings such as retinal structural changes in age-related macular degeneration[9] or hyper-reflective foci,[33,36] cystoid space,[27] microaneurysm,[37] and degenerated photoreceptor layers in diabetic macular edema.[33] Evaluation of parallelism will be tested in retinal diseases other than ERM and using different OCT machines in future.

Our study has the following limitations: (1) sample size was relatively small; and (2) there is room for improvement in the filtering process.

In conclusion, parallelism is proposed as a new robust and practical parameter for structural integrity. This parameter reflects how parallel the layers are to each other in OCT images. Parallelism was significantly lower in eyes with ERM than in normal eyes, and correlated strongly with metamorphopsia and visual acuity in eyes with ERM.

ALL AUTHORS HAVE COMPLETED AND SUBMITTED THE ICMJE FORM FOR DISCLOSURE OF POTENTIAL CONFLICTS OF INTEREST and none were reported. The authors indicate no funding support. Contributions of authors: design of the study (A.U., T.M., K.O., N.Y.); conduct of the study (A.U., T.M., N.U., K.O., K.N., S.Y., Y.D., N.Y.); collection, management, analysis, and interpretation of the data (A.U., T.M., N.U., K.O., K.N., S.Y., Y.D., N.Y.); preparation, review, or approval of the manuscript (A.U., T.M., N.U., K.O., K.N., S.Y., Y.D., N.Y.).

REFERENCES

1. Huang D, Swanson EA, Lin CP, et al. Optical coherence tomography. *Science* 1991;254(5035):1178–1181.
2. Stopa M, Bower BA, Davies E, Izatt JA, Toth CA. Correlation of pathologic features in spectral domain optical coherence tomography with conventional retinal studies. *Retina* 2008;28(2):298–308.
3. Koizumi H, Spaide RF, Fisher YL, Freund KB, Klancnik JM Jr, Yannuzzi LA. Three-dimensional evaluation of vitreomacular traction and epiretinal membrane using spectral-domain optical coherence tomography. *Am J Ophthalmol* 2008; 145(3):509–517.
4. Georgopoulos M, Geitzenauer W, Ahlers C, Simader C, Scholda C, Schmidt-Erfurth U. [High-resolution optical coherence tomography to evaluate vitreomacular traction before and after membrane peeling]. *Ophthalmologe* 2008; 105(8):753–760.
5. Hee MR, Puliafito CA, Wong C, et al. Quantitative assessment of macular edema with optical coherence tomography. *Arch Ophthalmol* 1995;113(8):1019–1029.
6. Parravano M, Oddone F, Boccassini B, et al. Reproducibility of macular thickness measurements using Cirrus SD-OCT in neovascular age-related macular degeneration. *Invest Ophthalmol Vis Sci* 2010;51(9):4788–4791.
7. Kiernan DF, Mieler WF, Hariprasad SM. Spectral-domain optical coherence tomography: a comparison of modern high-resolution retinal imaging systems. *Am J Ophthalmol* 2010;149(1):18–31.
8. Sakamoto A, Hangai M, Yoshimura N. Spectral-domain optical coherence tomography with multiple B-scan averaging for enhanced imaging of retinal diseases. *Ophthalmology* 2008;115(6):1071–1078.e1077.
9. Fleckenstein M, Charbel Issa P, Helb HM, et al. High-resolution spectral domain-OCT imaging in geographic atrophy associated with age-related macular degeneration. *Invest Ophthalmol Vis Sci* 2008;49(9):4137–4144.
10. Yamaike N, Tsujikawa A, Ota M, et al. Three-dimensional imaging of cystoid macular edema in retinal vein occlusion. *Ophthalmology* 2008;115(2):355–362.e352.
11. Forooghian F, Stetson PF, Meyer SA, et al. Relationship between photoreceptor outer segment length and visual acuity in diabetic macular edema. *Retina* 2010;30(1):63–70.
12. Inoue M, Morita S, Watanabe Y, et al. Inner segment/outer segment junction assessed by spectral-domain optical coherence tomography in patients with idiopathic epiretinal membrane. *Am J Ophthalmol* 2010;150(6):834–839.
13. Okamoto F, Sugiura Y, Okamoto Y, Hiraoka T, Oshika T. Associations between metamorphopsia and foveal microstructure in patients with epiretinal membrane. *Invest Ophthalmol Vis Sci* 2012;53(11):6770–6775.
14. Kim JH, Kang SW, Kong MG, Ha HS. Assessment of retinal layers and visual rehabilitation after epiretinal membrane removal. *Graefes Arch Clin Exp Ophthalmol* 2013;251(4): 1055–1064.
15. Nukada M, Hangai M, Mori S, et al. Detection of localized retinal nerve fiber layer defects in glaucoma using enhanced spectral-domain optical coherence tomography. *Ophthalmology* 2011;118(6):1038–1048.
16. Morooka S, Hangai M, Nukada M, et al. Wide 3-dimensional macular ganglion cell complex imaging with spectral-domain optical coherence tomography in glaucoma. *Invest Ophthalmol Vis Sci* 2012;53(8):4805–4812.
17. Hirashima T, Hangai M, Nukada M, et al. Frequency-doubling technology and retinal measurements with spectral-domain optical coherence tomography in preperimetric glaucoma. *Graefes Arch Clin Exp Ophthalmol* 2013; 251(1):129–137.
18. Murakami T, Nishijima K, Akagi T, et al. Segmentational analysis of retinal thickness after vitrectomy in diabetic macular edema. *Invest Ophthalmol Vis Sci* 2012;53(10):6668–6674.
19. Krebs I, Hagen S, Smretschnig E, Womastek I, Brannath W, Binder S. Reproducibility of segmentation error correction in age-related macular degeneration: Stratus versus Cirrus OCT. *Br J Ophthalmol* 2012;96(2):271–275.
20. Takayama K, Hangai M, Durbin M, et al. A novel method to detect local ganglion cell loss in early glaucoma using spectral-domain optical coherence tomography. *Invest Ophthalmol Vis Sci* 2012;53(11):6904–6913.
21. Wanek J, Zelkha R, Lim JI, Shahidi M. Feasibility of a method for en face imaging of photoreceptor cell integrity. *Am J Ophthalmol* 2011;152(5):807–814.e801.
22. Yang Q, Reisman CA, Chan K, Ramachandran R, Raza A, Hood DC. Automated segmentation of outer retinal layers in macular OCT images of patients with retinitis pigmentosa. *Biomed Opt Express* 2011;2(9):2493–2503.
23. Tilleul J, Querques G, Canoui-Poitrine F, Leveziel N, Souied EH. Assessment of a spectral domain OCT segmentation software in a retrospective cohort study of exudative AMD patients. *Ophthalmologica* 2013;229(2):80–85.
24. Ooto S, Hangai M, Takayama K, et al. High-resolution imaging of the photoreceptor layer in epiretinal membrane using adaptive optics scanning laser ophthalmoscopy. *Ophthalmology* 2011;118(5):873–881.
25. Yoneda A, Higaki T, Kutsuna N, et al. Chemical genetic screening identifies a novel inhibitor of parallel alignment of cortical microtubules and cellulose microfibrils. *Plant Cell Physiol* 2007;48(10):1393–1403.

26. Ueda H, Yokota E, Kutsuna N, et al. Myosin-dependent endoplasmic reticulum motility and F-actin organization in plant cells. *Proc Natl Acad Sci U S A* 2010;107(15):6894–6899.
27. Murakami T, Nishijima K, Sakamoto A, Ota M, Horii T, Yoshimura N. Foveal cystoid spaces are associated with enlarged foveal avascular zone and microaneurysms in diabetic macular edema. *Ophthalmology* 2011;118(2):359–367.
28. Canny J. A computational approach to edge detection. *IEEE Trans Pattern Anal Mach Intell* 1986;8(6):679–698.
29. Deriche R. Using Canny criteria to derive a recursively implemented optimal edge detector. *Int J Comput Vis* 1987;1(2):167–187.
30. Jacob M, Unser M. Design of steerable filters for feature detection using Canny-like criteria. *IEEE Trans Pattern Anal Mach Intell* 2004;26(8):1007–1019.
31. Zhang B, Zhang L, Zhang L, Karray F. Retinal vessel extraction by matched filter with first-order derivative of Gaussian. *Comput Biol Med* 2010;40(4):438–445.
32. Otsu N. A threshold selection method from gray-level histograms. *IEEE Trans Syst Man Cybern* 1979;9(1):62–66.
33. Uji A, Murakami T, Nishijima K, et al. Association between hyperreflective foci in the outer retina, status of photoreceptor layer, and visual acuity in diabetic macular edema. *Am J Ophthalmol* 2012;153(4):710–717, 717.e711.
34. Watanabe A, Arimoto S, Nishi O. Correlation between metamorphopsia and epiretinal membrane optical coherence tomography findings. *Ophthalmology* 2009;116(9):1788–1793.
35. Arimura E, Matsumoto C, Okuyama S, Takada S, Hashimoto S, Shimomura Y. Retinal contraction and metamorphopsia scores in eyes with idiopathic epiretinal membrane. *Invest Ophthalmol Vis Sci* 2005;46(8):2961–2966.
36. Bolz M, Schmidt-Erfurth U, Deak G, Mylonas G, Kriechbaum K, Scholda C. Optical coherence tomographic hyperreflective foci: a morphologic sign of lipid extravasation in diabetic macular edema. *Ophthalmology* 2009;116(5):914–920.
37. Horii T, Murakami T, Nishijima K, Sakamoto A, Ota M, Yoshimura N. Optical coherence tomographic characteristics of microaneurysms in diabetic retinopathy. *Am J Ophthalmol* 2010;150(6):840–848.

Biosketch

Akihito Uji, MD, PhD is an Assistant Professor of Ophthalmology at Kyoto University, Kyoto, Japan. He received his MD and PhD degrees from Okayama University Graduate School of Medicine, Okayama, Japan. His interests are diabetic retinopathy and image analysis studies.

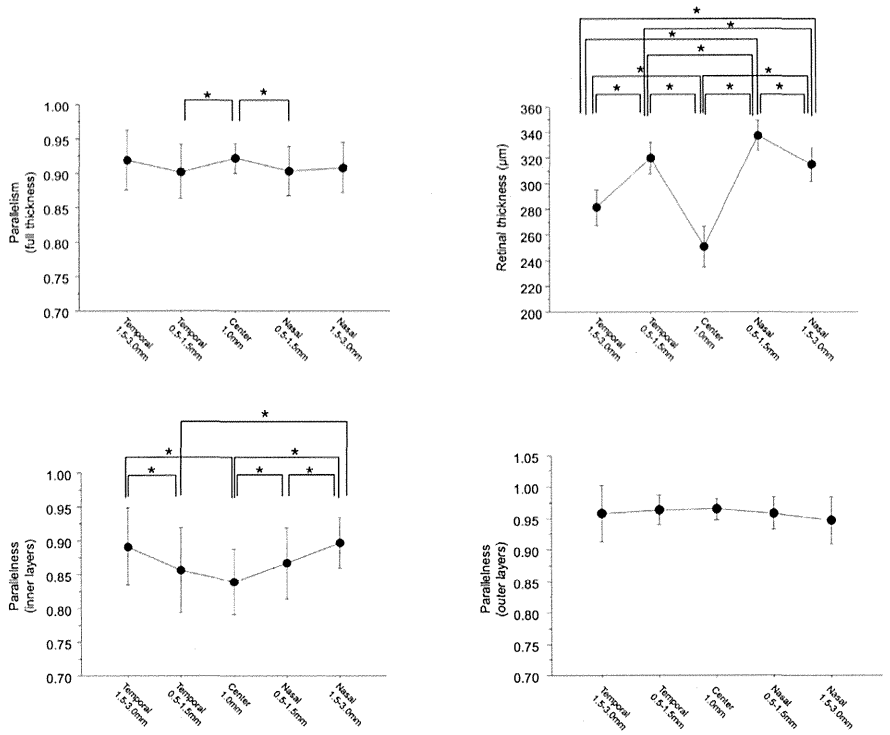

SUPPLEMENTAL FIGURE 1. Parallelism of retinal layers evaluated in horizontal line scan of normal subjects. (Top left) In the horizontal spectral-domain optical coherence tomography scan, significant differences were shown in full-thickness parallelism among 5 subfields (center [1 mm], 2 parafovea [temporal and nasal, 0.5-1.5 mm], and 2 perifovea [temporal and nasal, 1.5-3.0 mm]). (Top right) Retinal thickness was smallest in the center (1 mm) and was largest in the parafovea (0.5-1.5 mm). (Bottom left) Parallelism in the center (1 mm) was significantly smaller than those of the perifovea (1.5-3.0 mm) and parafovea (nasal, 0.5-1.5 mm) in the inner layer. (Bottom right) Significant differences were not shown in outer-layer parallelism among 5 subfields. *$P < .05$, paired t test followed by Bonferroni correction.

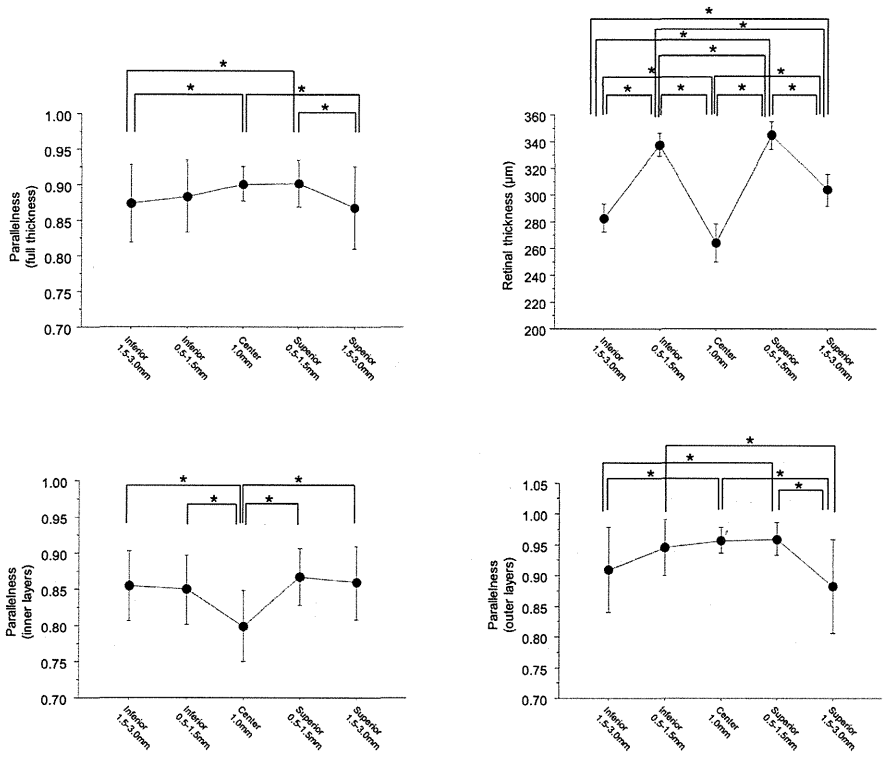

SUPPLEMENTAL FIGURE 2. Parallelism of retinal layers evaluated in vertical line scan of normal subjects. (Top left, Bottom left, Bottom right) In the vertical scan, significant differences were shown in full-thickness, inner-layer, and outer-layer parallelism. Parallelism of the perifovea (1.5-3.0 mm) tended to be smaller than parallelism of the other subfields, and significant differences in full-thickness and outer-layer parallelism were observed between the perifovea and some of the other subfields. Vessel shadows were imaged as lines perpendicular to the retinal layers in vertical scans, which might have caused decreased parallelism in the perifovea. (Top right) Retinal thickness was smallest in the center (1 mm) and was largest in the parafovea (0.5–1.5 mm). *$P < .05$, paired t test followed by Bonferroni correction.

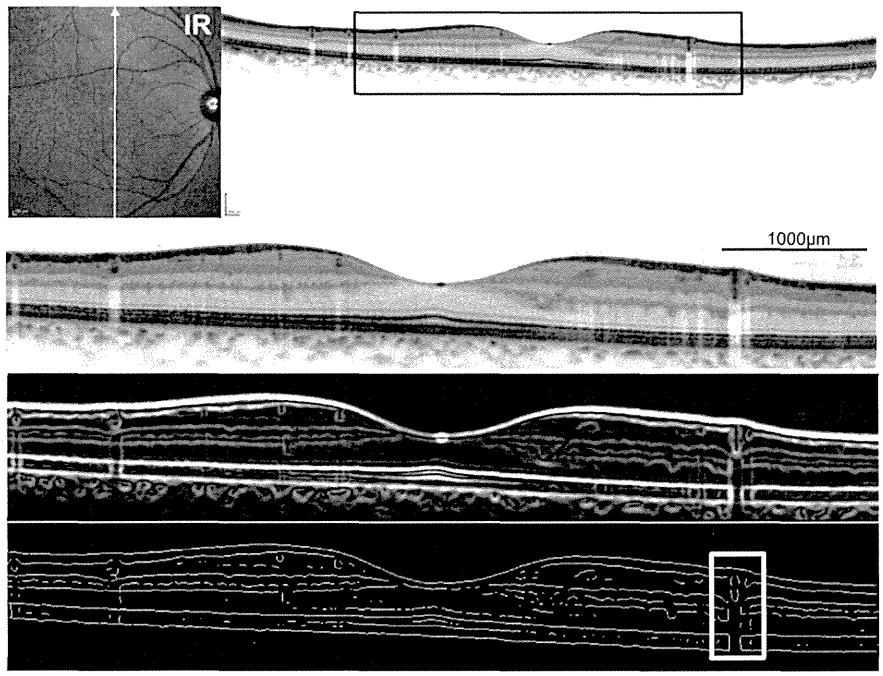

SUPPLEMENTAL FIGURE 3. Extraction of skeletonized image from retinal layers in vertical line scan of optical coherence tomographic images. Images of the right eye of a 65-year-old man from our database of normal volunteers. (Top row) Vertical line scan thorough the fovea of the infrared (IR) spectral-domain optical coherence tomography (SDOCT) image. (Second row) SDOCT image of the 6-mm section outlined in black in top row. (Third row) Filtered image of second row after application of derivative of a Gaussian filter for edge detection. (Bottom row) Skeletonized SDOCT image generated from third row. Note that vessel shadows are imaged as lines perpendicular to the retinal layers (outlined in white), which might have contributed to decreased parallelism in the perifovea (inferior, 1.5-3.0 mm) compared with the horizontal scan. Parallelism calculated for the 6-mm section, full thickness of the center (1 mm), parafovea (superior, 0.5-1.5 mm), and perifovea (superior, 1.5-3.0 mm) was 0.844, 0.928, 0.885, and 0.784, respectively.